Bioinspiration & Biomimetics

PAPER

Smooth transition for CPG-based body shape control of a snake-like robot

To cite this article: Norzalilah Mohamad Nor and Shugen Ma 2014 *Bioinspir. Biomim.* **9** 016003

IOP Publishing Bioinspiration & Biomimetics

Bioinspir. Biomim. 9 (2014) 016003 (11pp) doi:10.1088/1748-3182/9/1/016003

Smooth transition for CPG-based body shape control of a snake-like robot

Norzalilah Mohamad Nor[1] and Shugen Ma[1,2]

[1] Department of Robotics, Ritsumeikan University, Japan
[2] School of Electrical Engineering and Automation, Tianjin University, China

E-mail: gr0119hx@ed.ritsumei.ac.jp and shugen@se.ritsumei.ac.jp

Received 1 August 2013
Accepted for publication 8 November 2013
Published 16 December 2013

Abstract

This paper presents a locomotion control based on central pattern generator (CPG) of a snake-like robot. The main point addressed in this paper is a method that produces a smooth transition of the body shape of a snake-like robot. Body shape transition is important for snake-like robot locomotion to adapt to different space widths and also for obstacle avoidance. By manipulating the phase difference of the CPG outputs instantly, it will results in a sharp point or discontinuity which lead to an unstable movement of the snake-like robot. To tackle the problem, we propose a way of controlling the body shape: by incorporating activation function in the phase oscillator CPG model. The simplicity of the method promises an easy implementation and simple control. Simulation results and torque analysis confirm the effectiveness of the proposed control method and thus, can be used as a locomotion control in various potential applications of a snake-like robot.

(Some figures may appear in colour only in the online journal)

1. Introduction

One of the interesting features of a natural snake is its body shape transition. Natural snakes will change their body shape depending on the space it travels. Therefore, our goal is to mimic the body shape transition feature into to a snake-like robot, to make it capable traveling in different types of space and to avoid obstacles online. The target is to switch motion patterns by simply tuning a single parameter. The basic idea of control is shown in figure 1.

The wave line in figure 1 is the shape movement of the snake robot where the number of *S*-shape of the snake robot increases or decreases depending on the space it travels or avoiding an obstacle. The amplitude transition of the body shape of the snake-like robot hence needs to be controlled during locomotion especially for rescue or searching purposes in hazardous or dangerous environments where the operation space is beyond human reached.

To control the locomotion of the snake-like robot, central pattern generator (CPG) is adopted because: (1) its computational cost is low, (2) it exhibits limit cycle behavior, and (3) its parameters have clear relationship with the output. CPG are neural networks that exist in spinal cords of living animals which are used as activation signal for muscle contractions in animals. The term computational cost means the computational complexity in finding the solution to a given task. There is no looping process in the algorithm such as the optimization algorithm (for example: genetic algorithm) which requires high internal memory of processor. On the other hand, the CPG model is well suited to be programmed on a microcontroller on board of the robot because of the direct relationship of the CPG parameters to the CPG output. The CPG mathematical model do not requires many steps and easy to be solved. According to [1] and [5], CPGs can produce rhythmic patterns without receiving any input or rhythmic/oscillatory inputs. Some examples of rhythmic activities are breathing and chewing. Further explanation on CPG can be found in [2–5, 24]. In control point of view, CPG-based control use dynamical systems of coupled nonlinear oscillators to generate the coordinated patterns of rhythmic output. By manipulating the CPG parameters, we can realize different gaits or locomotion patterns of bio-inspired robots such as hexapod, salamander and others. Locomotion control utilizing CPG model has been implemented into several types of mobile robots such as quadruped robot [6], amphibious robot [7], turtle-like robot [8], and snake-like robot [9].

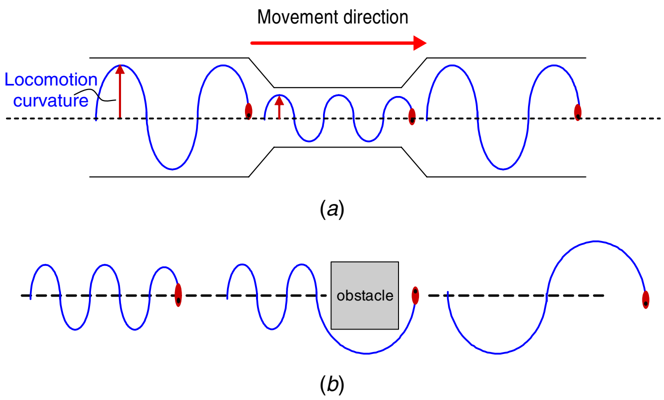

Figure 1. Illustration of snake movement: (*a*) in curvy pipe, (*b*) avoiding obstacle.

Most of researchers focus on controlling the locomotion of mobile robots when moving forward/backward with rhythmic movement patterns using CPG-based control. Zhu and Low [10] have designed locomotion control of a fish robot with fin propulsion. The CPG-based control method illustrates a way to switch motion patterns by simply tuning corresponding parameters. Crespi and Ijspeert [7] utilized CPG-locomotion control for online optimization of amphibious snake robot. Lu *et al* [11] analyze snake-like robot controlled by cyclic inhibitory CPG model where all the parameters of the CPG are fixed during the locomotion. Wu [12] improved the CPG connection model and analyzed the effect of CPG parameters to the CPG output without changing any parameters at any time instance. Tang and Ma [13], proposed a self-tuning multi phase CPG which enables the snake-like robot to adapt to environments. But switching locomotion mode from one type to another has yet being analyzed, plus the output signals show unstable wave when we change the CPG parameters online. All of these papers including [14–16] use predefined parameters to control the mobile robots.

To the authors' knowledge, most of the previous works done by other researchers do not consider transition of gaits or locomotion modes online especially for the body shape transition of a snake-like robot. From our analysis plus a review paper by Ijspeert [5], smooth transition between locomotion modes remain an open topic. For mobile robots, the common problem is the jerky movement that might occur due to the change of the control parameters. When the control parameters are instantly changed at random time, it will cause motion instability of the output wave. Chen *et al* [17] adopted three first-order low-pass filters to control the phase transition between gaits pattern of a hexapod robot. However, there is a change in amplitude and small deterioration of the output during the phase transition. To our knowledge, a small deterioration of CPG output waves will cause instability of robot's locomotion.

Due to the said problem of smooth locomotion transition, in this paper, we propose a way of controlling body shape of a snake-like robot, by introducing an activation function. We derive a simple mathematical function to control the phase transition of the CPG output, which results in the transition of the body shape of the snake-like robot. For our CPG model, we

Figure 2. Unidirectional coupling with four CPG oscillators.

have adopted phase oscillator to control the snake-like robot locomotion. The interesting property of this model is one of its parameter can be directly used to control the body shape of the snake-like robot.

This paper is organized as follows: firstly, in section 2, we will explain briefly about our CPG structure, the mathematical model used to control the locomotion curvature. Section 3 presents the analysis of our CPG unidirectional coupling structure, the effect and drawback by changing the phase instantaneously. Then, in section 4 we will explain the proposed method as mentioned before i.e., introducing an activation function. In section 5, we present simulation results, torque analysis and the control system design. In section 6, we will discuss the advantages and disadvantages in controlling the locomotion curvature using the proposed method. Finally, in section 7 we will draw some conclusions and our future tasks.

2. Network of CPG

2.1. Mathematical model

Nonlinear model of phase oscillator [2] has been utilized to control locomotion of our snake-like robot [18]. The mathematical model describing a system of one phase oscillator is as follows:

$$\dot{\theta}_i = 2\pi v_i + \sum w_{ij} \sin(\theta_j - \theta_i). \tag{1}$$

There is a constraint when using phase oscillator model, where w_{ij} needs to be large as compare to v_i to produce smooth output and to make the coupled oscillators synchronize at the same frequency with constant phase lag. For detail explanations, please refer to [18]. Due to this constraint, the oscillator model described in (1) has been modified to control the two parameters: v_i and w_{ij} simultaneously by introducing parameter τ, as follows:

$$\tau\dot{\theta}_i = 2\pi v_i + \sum w_{ij} \sin(\theta_j - \theta_i - \phi_{ij}). \tag{2}$$

Value of τ should be smaller than 1 to give effect to the output of CPG. The performance of the output will deteriorate when $\tau > 1$. With the control of parameter τ, we can always produce smooth output by maintaining the range of v_i and w_{ij}. The output for each oscillator is defined as follow:

$$\begin{aligned} x_i &= A\cos(\theta_i) \\ \text{joint\_angle}[i] &= x_i \end{aligned} \tag{3}$$

where x_i is the ith joint angle. Descriptions of parameter of our CPG model is explained in table 1.

2.2. Structure of CPG

In this section, we will introduce a simple CPG structure to control the snake-like robot locomotion so-called unidirectional coupling as shown in figure 2. Further

Table 1. Description of the CPG parameters.

Items	Details
θ_i	Phase of the ith oscillator
θ_j	Phase of the jth oscillator
υ_i	Intrinsic frequency
A	Amplitude
w_{ij}	Coupling weights between oscillators
ϕ_{ij}	Phase bias
x_i	Rhythmic and positive output signal
$\dot{\theta}_i$	Determination of the time evolution of the phase θ_i
τ	Frequency control

explanation on our proposed CPG structure can be referred in [18]. There is an interesting feature of this CPG structure, where we can easily utilize parameter ϕ_{ij} to control phase difference between the CPGs. For our CPG-based locomotion control, the value of parameter ϕ is the same for all oscillators to control the number of S-shape of the snake-like robot with symmetric locomotion. To obtain a symmetric locomotion, constant phase difference between oscillators is required and this can be achieved by setting the same value of ϕ for all oscillators. Throughout this paper, we will use $-\phi$ for descending connection and $+\phi$ for ascending connection.

It should be noted that, all oscillators should have input of θ_j, where θ_j is the phase of the neighboring oscillator. After thorough analysis in [18], the first oscillator (joint 1) should receive feedback from the second oscillator to achieve constant phase difference for all oscillators. The parameter ϕ of the phase oscillator shows a clear relation to the CPG output. Using the proposed structure of unidirectional coupling, the total phase difference, ϕ_{total} is given as follows:

$$\phi_{\text{total}} = n\phi \tag{4}$$

where n is the number of actuated joints from head to tail of the snake-like robot. Herein, to produce one S-shape locomotion, the total phase difference should be equal to 2π. Thus, number of locomotion of S-shape, N can be given as:

$$N = n\phi/2\pi. \tag{5}$$

By modifying the value of ϕ, we can obtain the desired serpentine locomotion of the snake-like robot, where (5) can be rearranged as follows:

$$\phi = 2\pi N/n. \tag{6}$$

2.3. Conversion of CPG signal to joint angle

From the previous subsection, we have already described that, one CPG signal will control one joint angle of the snake-like robot. In order to realize a serpentine locomotion of a natural snake, a snake-like robot is designed to have number of units connected to each other by a rotational joint. Following figure 3 shows a typical design of a snake-like robot where the joint angle between the snake units is controlled by our proposed CPG signal.

The setting of parameter ϕ is essential to achieve the desired S-shape locomotion, where each of the CPG output signal, x_i, will be sent to the joint motor of the snake-like robot as a joint angle to realize the desired S-shape.

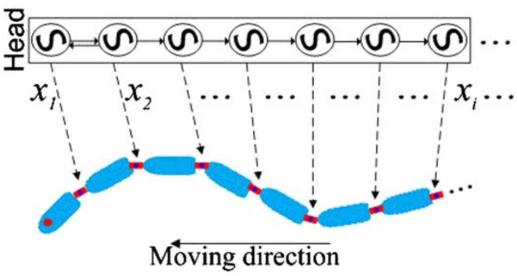

Figure 3. CPG signal implemented to control the joint angle of a snake-like robot.

3. Analysis of the CPG model

In this section, we will illustrate the output of the proposed unidirectional coupling and the way to control the parameter ϕ in relation to the body shape of the snake-like robot. Here, we use $\phi = -\pi/3$ for descending connection and $\phi = \pi/3$ for ascending connection in the simulation shown in figure 4.

3.1. Output of CPGs

Using the proposed unidirectional coupling of CPGs, we can obtain a direct relationship between parameter ϕ and the output of the CPGs, x_i. This clear relationship makes the locomotion control of the snake-like robot become easy by just manipulating the parameter ϕ. Firstly, we will show the behavior of θ_i and x_i for each of the CPGs (see figure 4).

Figure 4(a) shows the behavior of θ_i for four CPGs output. It can be deduced that ϕ is the phase difference between each of the CPGs and as ϕ is increased, the phase difference between CPGs will also increase. Thus, we can easily manipulate ϕ to control the number of S-shape of the snake-like robot locomotion.

3.2. Phase transition

Here, the effect of manipulating value of ϕ instantly at random time is analyzed. Since the goal is to change the snake-like robot locomotion online, first, we need to investigate the behavior of the CPGs output during the ϕ transition. Figure 5 shows the simulation results while ϕ is changed from $\pi/4$ to $\pi/2$. For easy view, we just show the results of two outputs of the CPGs.

Referring to figure 5, the outputs of CPGs produce sharp curve or discontinuity during the transition of ϕ from $\pi/4$ to $\pi/2$ at time = 5 s. This non-smooth transition is due to the sudden change of ϕ. Thus, manipulating ϕ directly for the locomotion control might damage the joint motor of the snake-like robot.

There are two main problems of the phase transition: (1) there is a sharp edge at the transition as shown in figure 5, and (2) there is more than one CPGs output to control the snake-like robot, which produces different behavior of curve at the transition point, as shown in figure 6. The transition point is defined as the point where the phase transition starts.

The curve is continuous but it has a visible crease which is unacceptable for locomotion of a snake-like robot. This sharp

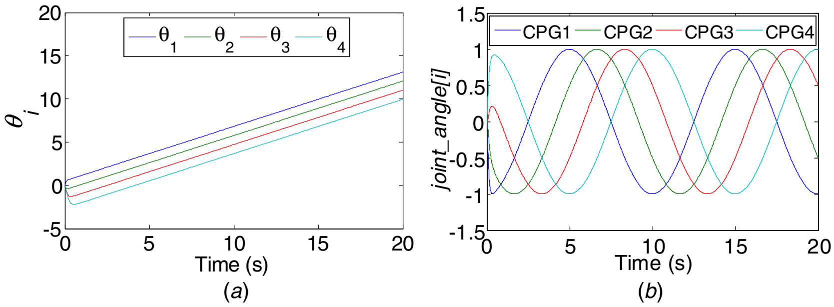

Figure 4. Behavior of CPGs at $\phi = \pi\ /3$: (*a*) θ_i with respect to time, (*b*) effect of θ_i to the CPGs output x_i.

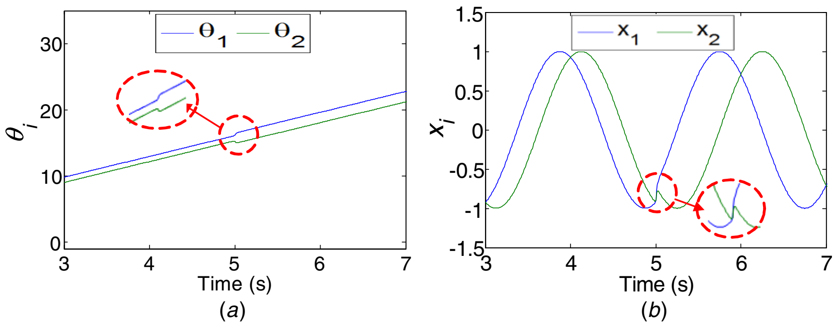

Figure 5. Behavior of CPGs when ϕ is changed from $\pi/4$ to $\pi/2$ at time 5 s: (*a*) θ_i with respect to time, (*b*) effect of θ_i to the CPGs output x_i.

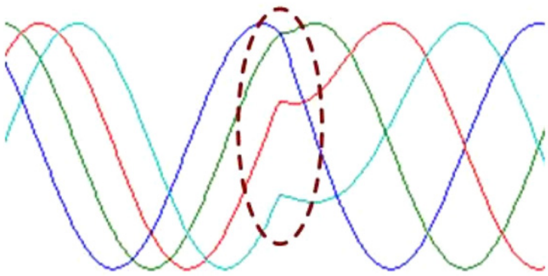

Figure 6. Different behavior of CPG outputs at the transition point.

join will results in sudden change with unstable movement of the locomotion of the snake-like robot.

4. Criteria of desired continuity and smoothness of locomotion

This section will discuss the definition of continuity and smoothness of the desired CPGs output curve. The measurement of continuity and smoothness of a curve is based on parametric continuity, C_n and geometric continuity, G_n. Geometric continuity requires the geometry to be continuous, while parametric continuity requires that the underlying parameterizations be continuous as well. Further explanation on the continuity can be found in [20]. In our case, the degree of smoothness that we desire for our snake-like robot locomotion is at least C_2 and G_2. It is easy to check that the CPGs output is always 0th-order continuity, C_0 and G_0. To analyze C_1 of (2), we need to calculate its derivative with respect to time, t. Thus, by using a chain rule, the derivative of (2) is obtained as follows:

$$\tau\ddot{\theta}_i = -w_{ij}[\dot{\theta}_i\cos(\theta_j - \theta_i - \phi_{ij})] \tag{7}$$

and we differentiate again (7) with respect to t, to analyze C_2:

$$\tau\ \dddot{\theta}_i = w_{ij}\big[\big[\dot{\theta}_i^2\cos(\theta_j - \theta_i - \phi_{ij})\big] - \ddot{\theta}\cos(\theta_j - \theta_i - \phi_{ij})\big]. \tag{8}$$

From (7) and (8), it can be directly figured out that the two equations does not imply C_1 and C_2 by substituting $\phi_{ij} = \phi_1$ before the phase transition and $\phi_{ij} = \phi_2$ after the phase transition.

Additionally, the curve of the CPGs output produces a kink during the phase transition (refer figure 5(*b*)), it does not imply G_1 and G_2 as well, because the tangent direction changes discontinuously at the kink. In figure 7, we define the criteria of a smooth curve based on the geometric continuity. In the next subsection, we will propose an approach to solve the addressed phase transition problem.

5. A method for smooth phase transition—introducing an activation function

In previous section, we have already shown the effect of manipulating parameter ϕ instantly. As a result of the sudden change of ϕ, the output of CPGs will not be smoothed, which causes an unstable movement of the snake-like robot. Thus, we introduce a method to control the phase transition by introducing an activation function. For simplicity, we have selected linear bipolar as our activation function, where ϕ change linearly with respect to time during the phase transition.

The linear bipolar has been selected as activation function for smooth phase transition because of its output behavior that is linearly increased with the independent variable. Figure 8 illustrates the main idea of manipulating ϕ from ϕ_1 to ϕ_2

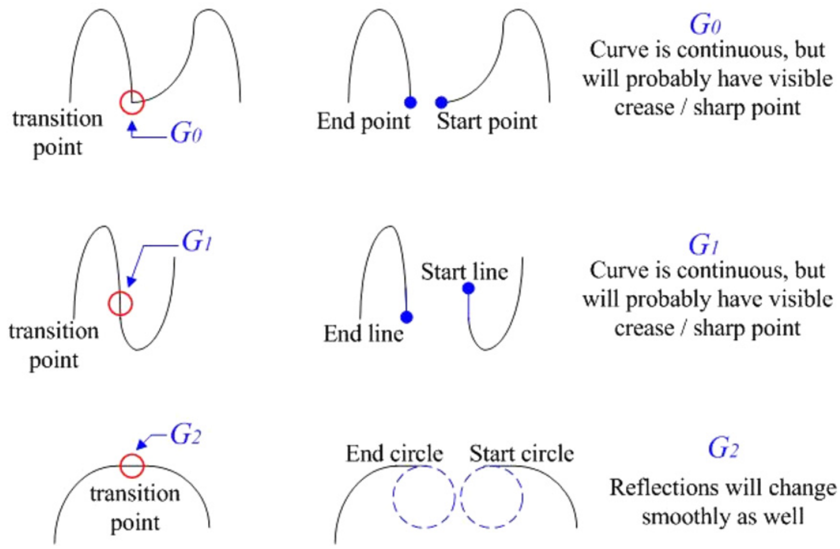

Figure 7. Description of geometric continuity for G_0, G_1 and G_2.

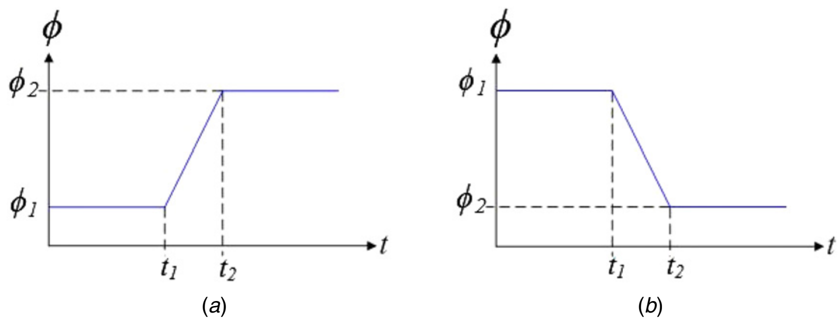

Figure 8. Linear bipolar: (*a*) ϕ linearly increase, (*b*) ϕ linearly decrease.

as time t increases from t_1 to t_2. ϕ can be either increased or decreased as time increases. We will derive a general mathematical model that describes both situations as depicted in figure 8(*a*) and (*b*).

The mathematical model that describes relationship between ϕ and time, t so that at t_1, ϕ is ϕ_1 and at t_2, ϕ will be ϕ_2 is as follows:

$$\phi = \phi_1 - \alpha(t_1 - t) \tag{9}$$

$$\alpha = \phi_1(N_2/N_1)(1 - (N_1/N_2))/(t_2 - t_1) \tag{10}$$

where

$$\phi = \begin{cases} \phi_1 & t \leqslant t_1 \\ \phi_1 - \alpha(t_1 - t) & t_1 < t < t_2 \\ \phi_2 & t \geqslant t_2. \end{cases} \tag{11}$$

Details derivation of (9) and (10) are given in appendix A. From (9), the *S*-shape locomotion can be easily controlled by substituting the desired value of N_2. The parameters ϕ_1 and N_1 are all predefined constant values. $(t_2 - t_1)$ is the transition time of the phase difference ϕ_1 to ϕ_2. t_1 is the trigger time for the phase transition.

5.1. Analysis of parametric continuity

To begin, the analysis should be divided into two parts because it is a piecewise linear activation function. The first part is at $t = t_1$, while the second part is at $t = t_2$. To analyze C_1 properties, we refer to (7). For the first part of the analysis, we substitute ϕ_1 into (7):

$$\tau\ddot{\theta}_i = -w_{ij}[\dot{\theta}_i \cos(\theta_j - \theta_i - \phi_1)]. \tag{12}$$

Then, we substitute (9) into (7):

$$\tau\ddot{\theta}_i = -w_{ij}[\dot{\theta}_i \cos(\theta_j - \theta_i - (\phi_1 - \alpha(t_1 - t)))] \tag{13}$$

at $t = t_1$, we obtain:

$$\tau\ddot{\theta}_i = -w_{ij}[\dot{\theta}_i \cos(\theta_j - \theta_i - \phi_1)]. \tag{14}$$

For the second part of the analysis, we repeat the same procedure as the first part of the analysis at $t = t_2$, and obtain the following:

$$\tau\ddot{\theta}_i = -w_{ij}[\dot{\theta}_i \cos(\theta_j - \theta_i - \phi_2)] \tag{15}$$

for both left-hand side and right-hand side of t_2.

The analysis of the C_2 continuity is similar with the C_1 continuity, using (8), where we can directly obtain the following:

$$\tau\,\dddot{\theta}_i = w_{ij}\left[\left[\dot{\theta}_i^2 \cos(\theta_j - \theta_i - \phi_2)\right] - \ddot{\theta}\cos(\theta_j - \theta_i - \phi_2)\right] \tag{16}$$

for both left-hand side and right-hand side at both t_1 and t_2.

The results directly clarify the C_1 and C_2 continuity of the piecewise activation function.

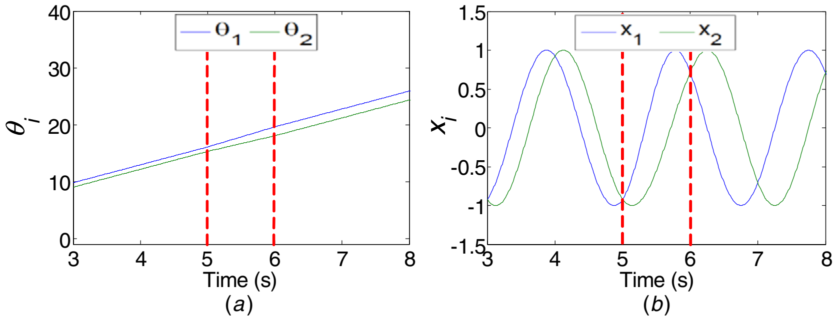

Figure 9. Behavior of CPGs when ϕ is changed from $\pi/4$ to $\pi/2$: (*a*) θ_i with respect to time (*b*) output x_i.

5.2. Analysis of geometric continuity

Figure 9 shows the results of the output of CPGs when applying the derived linear bipolar function (9) into our CPG model. There is a smooth linear changed during the ϕ transition. In this simulation, we use $\phi_1 = \pi/4$, $\phi_2 = \pi/2$, $n = 8$, and $t_2 - t_1 = 1$ s. Here, ϕ_1 corresponds to $N_1 = 1$, and ϕ_2 corresponds to $N_2 = 2$.

By incorporating our proposed activation function, we can obtain smooth linear change of the CPGs output. In figure 9, at transition time from 5 to 6 s, the output x_i changes smoothly with time.

In order to verify the desired geometric continuity, G_2 is achievable using our proposed method, we calculate the difference in slope of θ_i before and after the phase transition at two transition points: (1) the starting transition point, and (2) the end of the transition point. The general calculation is given as follows:

$$|\text{Slope}_{\text{before}} - \text{Slope}_{\text{after}}| \leqslant 0.01. \tag{17}$$

The criterion of '0.01' is randomly chose based on the time step use in the simulation, where the error is small enough to be ignored.

Based on the calculation at the two transition points, it is found that the difference in slope before and after the phase transition at the two transition points is less than 0.01, which met the set criterion. Also, it is known that the parametric continuity of order n implies geometric continuity of order n, and the C_n continuity has already been proved in the previous subsection. Hence, it is clarified that the proposed method for smooth phase transition achieves the desired geometric continuity, G_2.

6. Simulation results

For further verification, we had simulated the proposed mathematical model using open dynamic environment (ODE), where two passive wheels are adopted to each link to realize the swinging movement from side to side with ground asymmetric friction. Each of the snake unit is connected with joint actuator to drive the snake-like robot locomotion. Physical features of the snake-like robot are listed in table 2.

In the simulation, each joint is driven by an oscillator. The CPG outputs are used as angle inputs to the joints. The angle signal of the robot's joint, *joint_angle[i]* is calculated by

$$\text{joint\_angle}[i] = \beta x_i \tag{18}$$

Table 2. Physical parameters of simulated snake-like robot.

Items	Details
Snake unit	$S_u = 9$
Length of snake unit (m^3)	$0.05 \times 0.08 \times 0.14$
Weight of snake unit	$w = 0.1$ kg
Radius of wheel	$r_w = 0.06$ m
Thick of wheel	$t_w = 0.015$ m
Weight of wheel	$w_w = 0.01$ kg
Friction coefficient	$\mu_N = 0.5$; μ_T =0.01

where β is a gain from the control signal to the joint angle; and x_i is the output from ith oscillator.

6.1. Movement of the snake-like robot

Figure 10 shows the locomotion of simulated snake-like robot without applying the activation function.

The trace line in figure 10 shows the center of gravity trajectory of the head of the simulated snake-like robot. The trace line in the round-dash line in figure 10(*a*) and figure 10(*b*) shows clearly the sharp edge during the phase transition. There is a discontinuity in the forward movement of the robot, where the robot's direction is uncertain, which vigorously confirms the drawback of the direct phase transition.

In figure 11, the body shape of the snake-like robot change smoothly during transition of ϕ from $\pi/4$ to $\pi/2$ by incorporating the activation function. In figure 12, we invert the value ϕ from $\pi/2$ to $\pi/4$. For easy view, in figure 13, we show the trajectory of the head of the simulated snake-like robot during transition of ϕ from $\pi/2$ to $\pi/4$.

Based on the simulation results, we conclude that, it is essential to incorporate the activation function for phase transition to produce smooth locomotion of the snake-like robot.

6.2. Torque analysis

The smoothness transition of the CPG outputs are also affected the smoothness of the joint torque during the phase transition. The abrupt change of the phase will cause an abrupt change of the joint torque. We present the torque analysis for the first joint of the snake-like robot. Due to the symmetric gaits, it is expected that the torque results are almost the same for other joints. Please refer to appendix C for result of the middle joint torques.

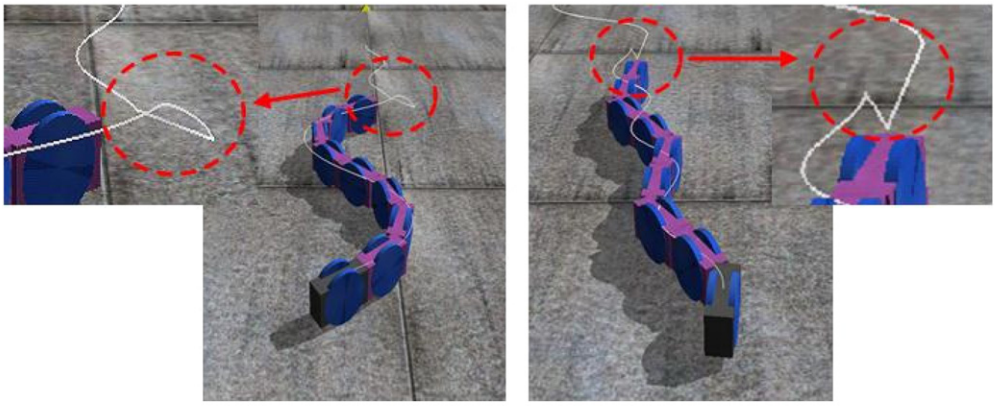

(*a*) (*b*)

Figure 10. Locomotion of simulated snake-like robot with direct phase transition: (*a*) ϕ from $\pi/2$ to $\pi/4$, (*b*) ϕ from $\pi/4$ to $\pi/2$.

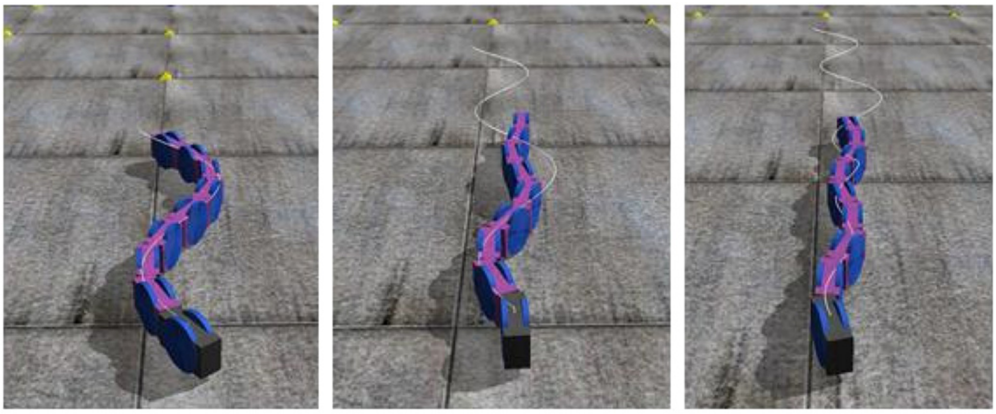

(*a*) (*b*) (*c*)

Figure 11. Simulation result of snake-like robot locomotion using activation function: (*a*) $\phi = \pi/4$ (*b*) transition of ϕ from $\pi/4$ to $\pi/2$ (*c*) $\phi = \pi/2$.

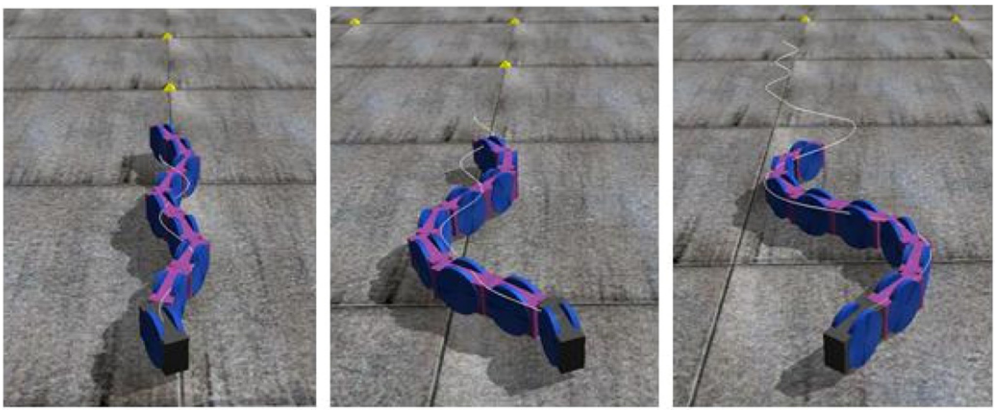

(*a*) (*b*) (*c*)

Figure 12. Simulation result of snake-like robot locomotion using activation function: (*a*) $\phi = \pi/2$ (*b*) transition of ϕ from $\pi/2$ to $\pi/4$ (*c*) $\phi = \pi/4$.

From our analysis, the torque will be affected by the transition of phase due to the stability of the CPG outputs before reaching the phase locking state. When the CPG outputs are perturbed, it needs time to converge to its steady state. In figure 14, at the initial stage (time < 0.2 s), there is a peak in the torque profile. This is because the CPG has yet reached its steady state (i.e., the CPG has yet converged to its limit cycle). During the transition of the phase (between time 5 to 6 s, figure 14(*b*)), there is a small fluctuation due to the perturbation (change in the value of the CPG parameter). The small fluctuation is due to the linear parameter change of the ϕ with time (because the linear bipolar activation function is incorporated). Conversely, in figure 14(*a*), the sudden change of the ϕ results a high peak of torque during the transition.

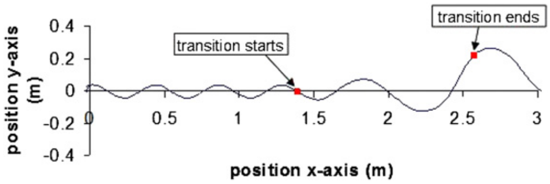

Figure 13. Simulation result of trajectory of snake-like robot locomotion: transition of ϕ from $\pi/2$ to $\pi/4$.

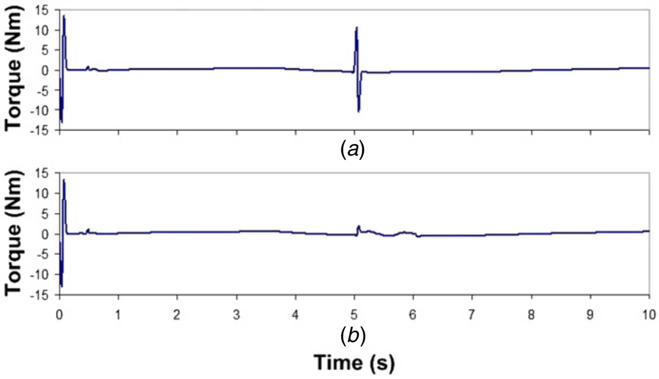

Figure 14. Torque of the first joint for transition of ϕ from $\pi/4$ to $\pi/2$: (*a*) direct transition (*b*) with activation function.

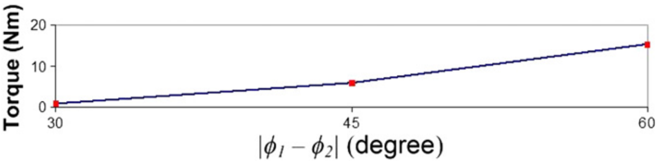

Figure 15. Maximum torque generated on the first joint for $|\phi_1 - \phi_2|$ without activation function (direct phase transition).

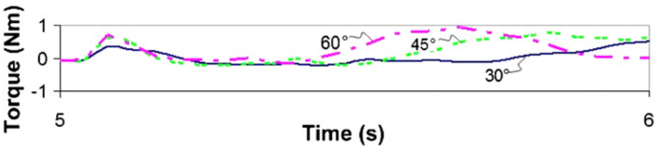

Figure 16. Behavior of torque of the first joint during phase transition for $|\phi_1 - \phi_2|$ with activation function, the transition time is between 5 to 6 s.

In figure 15, we show the maximum torque generated by the first joint for different $|\phi_1 - \phi_2|$ with direct phase transition, which results in nonlinear profile. As the difference between ϕ_1 and ϕ_2 gets larger, it produces higher peak of the torque. The reason behind this is due to the sudden and large change from the initial position to its new position. The larger the change of the slope of θ_i after the phase transition, the larger the peak of the torque produces during the phase transition.

On the contrary, by incorporating the activation function, the change of the torque is nearly constant between 1 to -1 Nm for various value of $|\phi_1 - \phi_2|$ (please refer figure 16). This is due to the linear change of the ϕ which directly affects the output of the CPG. By comparing the torque results between the direct phase transition and the activation function approach, we prove that the activation function approach gives nearly a constant torque during the phase transition.

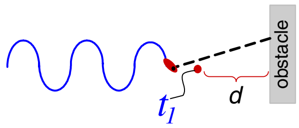

Figure 17. Schematic of sensor-based obstacle avoidance.

6.3. Control system design

We can apply the control of the body shape transition into a snake-like robot to move into a different space width or to avoid an obstacle, as shown in figure B1 in appendix B. For instance, IR sensors can be installed at the head of the snake-like robot, or at the side of its body depending on the application. The trigger of the phase transition is t_1 with appropriate N_2.

To set the parameter of (9), $(t_2 - t_1)$ is set to 1s (this value is selected based on in depth analysis), where the value is the minimum value to obtain a smooth phase transition without any jerky movement of the snake-like robot. In figure 17, d is the distance from the obstacle to the starting of the phase transition, t_1. The distance should be in appropriate length to ensure the snake-like robot is totally changed to its final *S*-shape, N_2. In the simulation environment (figure B1), the parameters t_1 and N_2 are calculated directly from the obstacle and the head of the snake-like robot.

The control system design of the snake-like robot is shown in figure 18(*a*). Bus communication (e.g. I2C, CAN, SPI) can be used to perform the connection of the CPG network. One MCU will control one robot's joint. The calculated CPG signal inputs to the PWM to drive the joint's motor. Figure 18(*b*) shows the flow chart of the CPG-controlled process.

7. Discussion

Based on the simulation results, we conclude that by incorporating the activation function, smooth phase transition can be produced compared to direct transition at anytime instantly. Using the activation function, we can set any value of ϕ that corresponds to the desired number of *S*-shape. The advantage of this method is we can control the body shape of the snake-like robot at anytime by triggering t_1. With this advantage, we can plan whether to change the body shape before or during entering a different space width. This is the superiority over [25], where the bias can only be added when the signals is at zero point to avoid sudden change or discontinuity of the output signal.

Furthermore, the activation function is a simple linear piece-wise function. The derivation is done to achieve the main goal, i.e., to control one of the CPG parameter, ϕ in relation with the number of *S*-shape of the snake-like robot. The simplicity in controlling the smooth body shape transition promises a light computational cost, easy implementation, simple control and understandable by readers who may not familiar with CPG-based control. This idea is a preliminary work for potential applications in wave-based locomotion systems.

As shown in figure 6, the behavior at the transition point of each CPG output is different, depending on the transition

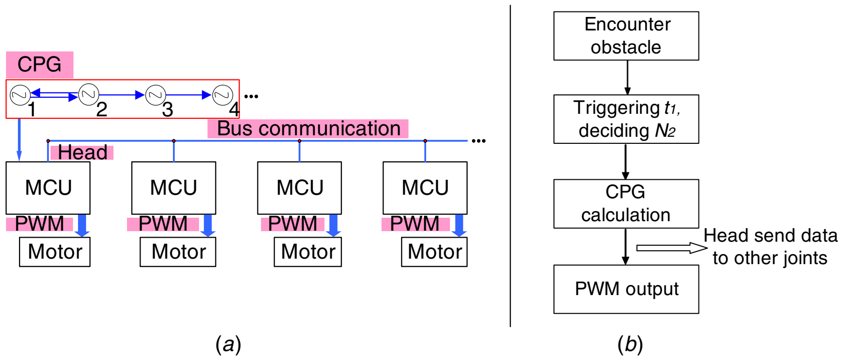

Figure 18. (*a*) Control system design, (*b*) flow chart of the CPG-controlled process.

point during the start of the phase transition. The CPG outputs produce an apparent kink as the transition point is away from the peak signal. Thus, the activation function is formulated to tackle the worst case of the discontinuous change in the tangent direction at the kink, which is at the middle or between the zero point to the peak point. Based on our analysis, parametric continuity C_2 and geometric continuity, G_2 are sufficient to obtain smoothness of robot's locomotion during the phase transition.

In addition, the fluctuation of the joint torque is in a small range and nearly constant for every $|\phi_1 - \phi_2|$ by implementing the activation function during the phase transition. Comparing with the direct phase transition, our proposed method produces good results of locomotion as well as the joint torque. Moreover, we found that the body shape curvature does not effect the torque except during the phase transition. With this, we know that the joint torque of the snake-like robot is not affected by the locomotion curvature. Therefore, the forward speed of the snake-like robot can be maintained during the locomotion.

However, right after the phase transition, we found that the direction of the snake-like robot deviates from its initial position (position before the phase transition starts). Based on initial analysis, the causes of the problems are due to: (1) slippery between the wheel and ground, (2) forward speed, (3) friction coefficient (surface parameter), (4) hardness of the ground, and (5) slip coefficients in tangential and normal direction. This is unacceptable for our snake-like robot locomotion during entering a narrow space because it may hit the wall or deviate from our desired path, but it is useful for obstacle avoidance. Currently, we still investigating the countermeasure for this problem.

8. Conclusions and future works

In this paper, we have proposed an approach to control the body shape of a snake-like robot by manipulating a single parameter, ϕ. By introducing an activation function during phase transition, we can get smooth movement of the snake-like robot. Simulation results confirmed the validity of our control method. There are two main conclusions: (1) the activation function can produce smooth phase transition, and (2) the body shape curvature does not effect the torque except during the phase transition.

Although we have successfully produced smooth change of the CPG outputs during phase transition, there is a problem that we encountered during our analysis. From our analysis by ODE simulations, we found that, after the phase transition, there is a small change of the direction of the snake-like robot. As our future work, we will investigate on how to encounter this problem so it would not effect our snake-like robot direction.

Appendix A

The derivation of a mathematical model for (7) and (8) that describes relationship between ϕ and time, t so that at t_1, ϕ is ϕ_1 and at t_2, ϕ will be ϕ_2 is as follows.

Step 1. Derive the relation between ϕ_1 and ϕ_2 by manipulating (6) : $n = 2\pi N / \phi$, we obtain:

$$\phi_1 = (N_1/N_2)\phi_2. \tag{A.1}$$

Step 2. Derive general equation for the linear bipolar.

Let the general equation be (*K and z are unknowns to be derived):

$$\phi = Kt + z. \tag{A.2}$$

At t_1:

$$z = \phi_1 - Kt_1. \tag{A.3}$$

At t_2:

$$z = \phi_2 - Kt_2. \tag{A.4}$$

Substitute (A.1) into (A.3):

$$z = (N_1/N_2)\phi_2 - Kt_1. \tag{A.5}$$

Equate (A.4) and (A.5):

$$\phi_2 - Kt_2 = (N_1/N_2)\phi_2 - Kt_1. \tag{A.6}$$

Solving for K:

$$K = \phi_2(1 - (N_1/N_2))/(t_2 - t_1). \tag{A.7}$$

Substitute (A.7) into (A.3), and solve for z:

$$z = \phi_1 - [\phi_2(1 - (N_1/N_2))/(t_2 - t_1)]t_1. \tag{A.8}$$

Step 3. The linear bipolar function

let:

$$\alpha = \phi_1(N_2/N_1)(1 - (N_1/N_2))/(t_2 - t_1). \tag{A.9}$$

Finally we obtain:

$$\phi = \phi_1 - \alpha(t_1 - t). \tag{A.10}$$

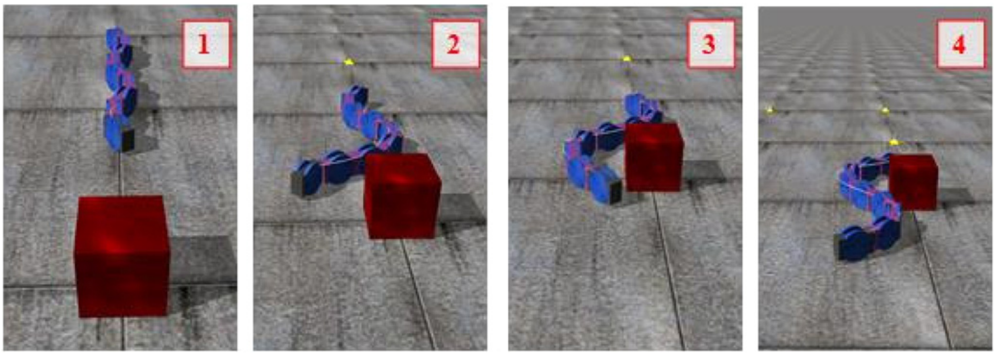

Figure B1. Potential application using our proposed body shape control: obstacle avoidance.

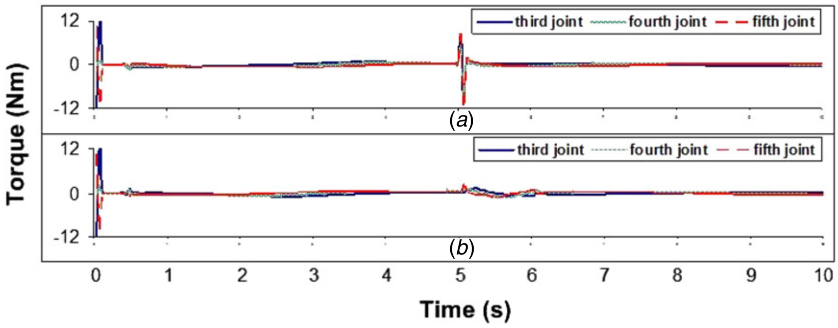

Figure C1. Torque of the middle joints when changing ϕ from $\pi/4$ to $\pi/2$: (*a*) direct transition (*b*) with activation function.

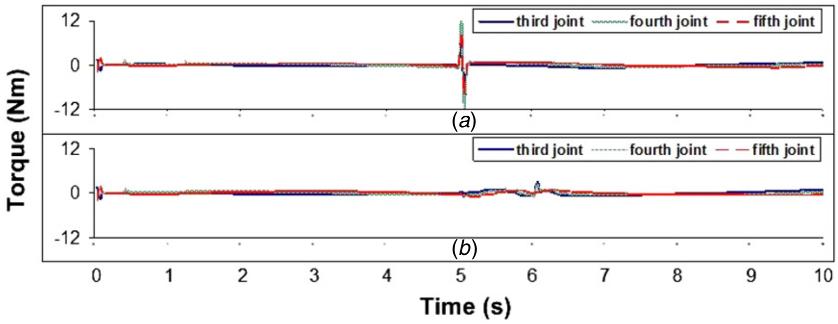

Figure C2. Torque of the middle joints when changing ϕ from $\pi/2$ to $\pi/4$: (*a*) direct transition (*b*) with activation function.

Appendix B

Currently, we are analyzing various potential applications of the proposed body shape control. This paper presents the preliminary works for our future application. Figure B1 shows an example of obstacle avoidance using our proposed control method.

Appendix C

For simplicity, we only show the torque results for the third, fourth and fifth joints of the snake-like robot locomotion. The results of all of the joint torques are approximately the same and overlap with each other. Figure C1 show the torque results when number of *S*-shape is changed from $N = 1$ to $N = 2$ (i.e., ϕ is changed from $\pi/4$ to $\pi/2$) and figure C2 shows the vice versa.

References

[1] Delcomyn F 1980 Neural basis for rhythmic behavior in animals *Science* **210** 492–8

[2] Cohen A H, Holmes P J and Rand R H 1982 The nature of coupling between segmental oscillators of the lamprey spinal generator for locomotion: a mathematical model *J. Math. Biol.* **13** 345–69

[3] Hooper S L 2000 Central pattern generators *Curr. Biol.* **10** 708–16

[4] MacKay-Lyons M 2002 Central pattern generation of locomotion: a review of the evidence *J. Am. Phys. Ther. Assoc.* **82** 69–83

[5] Ijspeert A J 2008 Central pattern generators for locomotion control in animals and robots: a review *Neural Netw.* **21** 642–53

[6] Liu C, Chen Q and Wang D 2011 CPG-inspired workspace trajectory generation and adaptive locomotion control for quadruped robots *IEEE Trans. Syst. Man Cybern.* **41** 867–80

[7] Crespi A and Ijspeert A J 2008 Online optimization of swimming and crawling in an amphibious snake robot *IEEE Trans. Robot.* **24** 75–87

[8] Seo K, Chung S J and Slotine J J E 2010 CPG-based control of a turtle-like underwater vehicle *Auton. Robots* **28** 247–69

[9] Wu X 2011 CPG-based neural controller for serpentine locomotion of a snake-like robot *Doctoral dissertation* Science and Engineering, Ritsumeikan University

[10] Zhou C and Low K H 2012 Design and locomotion control of a biomimetic underwater vehicle with fin propulsion *IEEE/ASME Trans. Mechatronics* **17** 25–35

[11] Lu Z, Ma S, Li B and Wang Y 2005 Serpentine locomotion of a snake-like robot controlled by musical theory *IEEE/RSJ Int. Conf. on Intelligent Robots and Systems (Edmonton, Canada)* pp 3019–24

[12] Wu X and Ma S 2009 CPG-based control of serpentine locomotion of a snake-like robot *Proc. 9th Int. IFAC Symp. on Robot Control (Gifu, Japan)* pp 871–6

[13] Tang C and Ma S 2011 A self-tuning multi-phase CPG enabling the snake robot to adapt to environments *IEEE/RSJ Int. Conf. on Intelligent Robots and Systems (San Francisco, USA)* pp 1869–74

[14] Prautsch P and Mita T 1999 Control and analysis of the gait of snake robots *IEEE Int. Conf. on Control Applications (Hawaii, USA)* pp 502–7

[15] Sprowitz A, Mockel R, Maye J, Asadpour M and Ijspeert A J 2007 Adaptive locomotion control in modular robots *Workshop on Self-reconfigurable Robots Systems and Applications IROS* pp 81–84

[16] Li B, Li Y and Rong X 2010 Gait generation and transitions of quadruped robot based on Wilson–Cowan weakly neural networks *Int. Conf. on Robotics and Biomimetics (Tianjin, China)* pp 19–24

[17] Chen W, Ren G, Zhang J and Wang J 2012 Smooth transition between different gaits of a hexapod robot via a central pattern generators algorithm *J. Intell. Robot. Syst.* **67** 255–70

[18] Nor N M and Ma S 2013 A simplified CPGS network with phase oscillator model for locomotion control of a snake-like robot *J. Intell. Robot. Syst.* August 2013

[19] Hirose S 1993 *Biologically Inspired Robot: Snake-Like Locomotors and Manipulators* (Oxford: Oxford University Press)

[20] Rogers D F 2000 *An Introduction to NURBS: With Historical Perspective* (San Francisco, CA: Morgan Kaufmann Publishers)

[21] Wrede R C and Spiegel M 2002 *Advanced Calculus* (New York: McGraw-Hill)

[22] Ijspeert A J, Crespi A, Ryczko D and Cabelguen J M 2007 From swimming to walking with a salamander robot driven by a spinal cord model *Science* **315** 1416–20

[23] Lepora N F, Verschure P and Prescott T J 2013 The state of the art in biomimetics *Bioinspir. Biomim.* **8** 013001

[24] Arena P, Fortuna L, Frasca M, Patan L and Vagliasindi G 2005 CPG-MTA implementation for locomotion control *ISCAS '05: IEEE Int. Symp. on Circuits and Systems (Kobe, Japan)* pp 4102–5

[25] Wu X and Ma S 2010 Autonomous collision-free behavior of a snake-like robot *IEEE Int. Conf. on Robotics and Biomimetics (Tianjin, China)* pp 1490–5